Characterization method of unusual second-order-harmonic generation based on vortex transformation

Chaojin Zhang,[1] Erheng Wu,[2] Mingliang Gu,[1] Zhengfeng Hu,[3] and Chengpu Liu[2,*]

[1]*School of Physics and Electronic Engineering, Jiangsu Normal University, Xuzhou 221116, China*

[2]*State Key Laboratory of High Field Laser Physics, Shanghai Institute of Optics and Fine Mechanics, Chinese Academy of Sciences, Shanghai 201800, China*

[3]*Key Laboratory of Quantum Optics, Shanghai Institute of Optics and Fine Mechanics, Chinese Academy of Sciences, Shanghai 201800, China*

(Received 26 June 2017; published 28 September 2017)

When a few-cycle laser beam nonresonantly propagates through an inversion-symmetric medium, beyond the usual odd-order harmonics in the transmission spectra, a well-defined spectral peak at twice the incident laser central frequency is disclosed [T. Tritschler *et al.*, Phys. Rev. Lett. **90**, 217404 (2003)]. Beyond the characterization method via the rf measurement of its carrier-envelope phase dependence, here a more direct mode of characterization is proposed by means of vortex transformation where a few-cycle vortex laser is adopted instead: One can easily clarify its origin as an usual third-order harmonic that appears to be a second-order harmonic, based on the criteria that the topological charge number of harmonics is directly proportional to its harmonic order.

DOI: 10.1103/PhysRevA.96.033854

As for strong laser interactions with media, it is well known that even-order harmonics cannot be supported if the media are spatial inversion symmetric. However, in the regime of extreme nonperturbative nonlinear optics with a Rabi energy comparable to the carrier photon energy [1], some unusual phenomena are disclosed as the result of resonant enhancement and wide spectral overlapping effects [2–7]. For example, a well-defined peak in the transmission spectra at twice the incident laser central frequency [ω_0, shown in Fig. 1(a)] is disclosed [5]. It seems to be second-order-harmonic generation (SHG), but this is not actually the case. Its origin has been clarified and experimentally confirmed by the rf measurement of its carrier-envelope phase (CEP) dependence [6] as the contribution of resonant enhancement way down in the low-energy tail of the spectrally broadened third harmonic, and thus it is in fact a third-harmonic-generation (THG) process disguised as SHG. The rf measurement scheme [5–7] used to clarify the peak's origin is based on the fact that, for an incident few-cycle pulse with a CEP of φ directly generated from a mode-locked laser oscillator, the induced usual SHG with a phase 2φ would lead to a beat note peak at a frequency of f_φ when beating with the fundamental laser, however, in the same spectral region, a peak at a frequency of $2f_\varphi$ is observed, and correspondingly the CEP dependence period is π rather than 2π.

Beyond the above characterization scheme [5–7] to the unusual SHG, one more convenient and direct mode of characterization is proposed here, and a corresponding numerical simulation via the solution of coupled Maxwell-Bloch equations confirms its feasibility. Compared with Refs. [5–7], here a few-cycle linearly polarized Laguerre-Gaussian (LG) vortex laser beam with a fundamental topological charge number of l [8–15] is used instead to investigate similar items. The time evolution and the spectral and transverse field distributions of the induced vortex harmonics are investigated, respectively, as shown in Figs. 1 and 2. In Fig. 1(a), a well-defined peak at twice the incident laser central frequency of ω_0 unexpectedly occurs for both topological charges of $l = 0$ (i.e., those investigated in Refs. [5,6]) and $l = 1$. By referring to the corresponding transverse field distributions [Figs. 2(c) and 2(d)] and based on the criteria that the topological charge number l_q of a qth-order harmonic is directly proportional to its harmonic order q, that is, $l_q = ql$ [11–15], the origin of this unusual SHG is in fact a THG [6]. Here, the word "unusual" means the SHG is not really a second harmonic, but is a THG that appears to be a SHG because its spectral position is at twice the incident laser frequency as the result of a resonant enhancement effect from the contribution of the low-energy long tail of the third harmonic, which could also be spectrally broadened by self-phase modulation. Beyond this simple characterization scheme, here, the propagation effects are also investigated, which show clear and significant distortions to this unusual SHG [Fig. 1(b)], but the propagation effects are unfortunately omitted in Refs. [5,6].

The schematic of the entire LG vortex laser interaction with media is described as follows: First, the LG beam, linearly polarized along the x direction, freely propagates in the vacuum from the left-hand side of the media along the z direction; then, when it arrives at the front surface of the media (at $z = 0$), it will partially reflect backwards, and most of it will penetrate the media and continue to propagate; finally, it exits from the media into the vacuum. At any position, one can record the temporal distributions of this laser field or other information. The initial incident LG pulse with a central frequency of ω_0, duration of τ_0, and CEP of φ is written as

$$\vec{E}(t=0,r,\phi,z) = E_{lp}\,\mathrm{sech}[1.76(z-z_0)/(c\tau_0)] \times \cos[\omega_0(z-z_0)/c+\varphi]\vec{e}_x. \quad (1)$$

*chpliu@siom.ac.cn

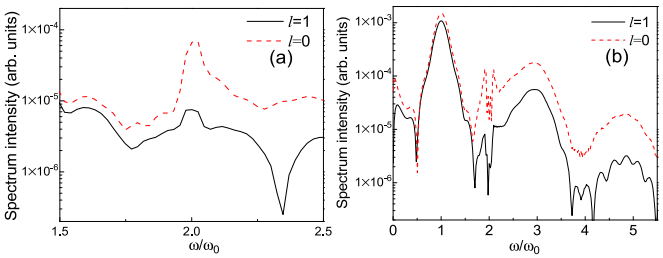

FIG. 1. Spectra of few-cycle LG pulses after a propagation distance of (a) 350 nm and (b) 8 μm, respectively. In (a), a well-defined peak at twice the incident laser central frequency of ω_0 unexpectedly occurs for both topological charges of $l = 0$ (dashed) and $l = 1$ (solid). In (b), the peak's intensity is obviously reduced and a dip occurs instead due to the propagation effects.

Here, the field amplitude E_{lp} is, with a specific definition [9], written as

$$E_{lp}(t=0,r,\phi,z) = \frac{E_0}{\left(1+\tilde{z}^2/z_R^2\right)^{1/2}}\left(\frac{r}{a(\tilde{z})}\right)^{|l|} L_p^{|l|} \times \left(\frac{2r^2}{a^2(\tilde{z})}\right)\exp\left(\frac{-r^2}{a^2(\tilde{z})}\right) \times \exp\left(\frac{-ikr^2\tilde{z}}{2\left(\tilde{z}^2+z_R^2\right)}\right)\exp(-il\phi) \times \exp\left(-i(2p+|l|+1)\tan^{-1}\frac{\tilde{z}}{z_R}\right), \quad (2)$$

with $\tilde{z} = z - z_0$ (z_0 is the initial laser peak position and a suitable choice of z_0 should ensure that the LG pulse penetrates negligibly into the media at $t = 0$ [16]) and $r = \sqrt{(x-x_0)^2+(y-y_0)^2}$ (x_0 and y_0 are the axial center coordinates on the transverse xy plane). $Z_R = \pi a_0^2/\lambda$ is the Rayleigh range and $a(\tilde{z})$ is the beam radius at $\tilde{z}$ with $a_0 = a(0)$ being the beam waist radius at z_0, which are both related to the characteristics of a Gaussian pulse with a central wavelength of λ. The most important term indicating the vortex property of the LG beams is $\exp(-il\phi)$ with a topological charge (TC) number of l ($l = 0, \pm1, \pm2, \ldots$), an azimuthal angle of ϕ, and a vortex laser helical phase of $l\phi$. In addition, $L_p^{|l|}$ is the associated Laguerre polynomial, where p denotes the transverse radial node number, which is assumed to be zero [9,15], E_0 is the peak amplitude of the electric field.

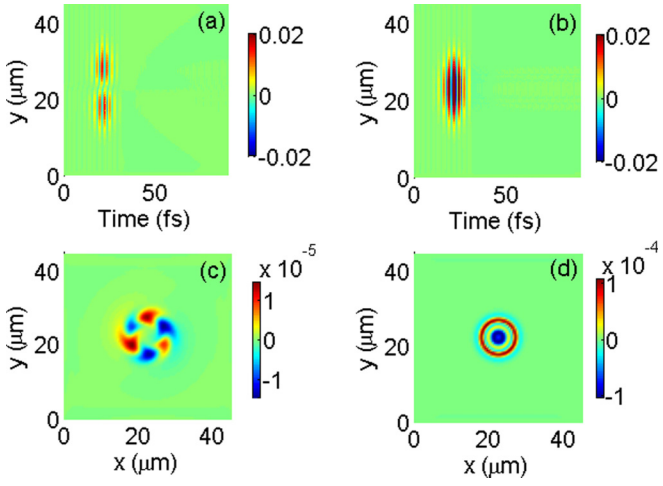

FIG. 2. Time evolutions of few-cycle LG pulses with a topological charge of (left) $l = 1$ and (right) $l = 0$ at a position of 350 nm within the medium but near to its front surface with $x = x_0$ μm (top). The corresponding transverse distributions of the unusual spectral peaks at $2\omega_0$ are also presented via the Gabor transformation with a suitable spectral width (bottom) at $t = 21.5$ fs.

The three-dimensional coupled Maxwell-Bloch (MB) equations describing the whole dynamics take the following forms [15],

$$\frac{\partial \vec{H}}{\partial t} = -\frac{1}{\mu_0}\nabla\times\vec{E}, \quad \frac{\partial \vec{E}}{\partial t} = \frac{1}{\varepsilon_0}\nabla\times\vec{H} - \frac{1}{\varepsilon_0}\frac{\partial \vec{P}}{\partial t}, \quad (3)$$

$$\frac{\partial \rho_{12}}{\partial t} = -i\left(\omega_{12}\rho_{12} + \frac{uE_x}{\hbar}n\right) - \frac{1}{\tau_1}\rho_{12}, \quad \frac{\partial n}{\partial t} = i\frac{2u}{\hbar}E_x(\rho_{12}-\rho_{12}^*) - \frac{1}{\tau_2}n. \quad (4)$$

Equations (3) are the Maxwell equations used for describing laser propagation, where $\vec{E}$ and $\vec{H}$ are electric or magnetic vectors. $\vec{P}$ is the macroscopic polarization as an emission source, and ε_0 and μ_0 are the vacuum permittivity and permeability, respectively. Equations (4) are the Bloch equations for describing the medium response to the induced laser, with ρ_{12} being the complex microscopic polarization (ρ_{12}^* is its complex conjugate) and $n = \rho_{22} - \rho_{11}$ the population difference between the two medium-energy levels with an energy difference of $\hbar\omega_{12}$ [15] and a dipole transition matrix moment of u. In addition, two important intrinsic time factors are the transverse dephasing time τ_1 and the longitudinal excited-state lifetime τ_2. In the following, $\tau_1 = 1.0$ ps and $\tau_2 = 0.5$ ps are assumed [4,15], much longer than the incident laser pulse duration (5 fs), which in fact can be neglected safely because of its trivial influence on the whole laser-matter interaction dynamics. The relation between $\vec{P}$ and ρ_{12} is $P_x = 2\,NuRe[\rho_{12}]$ with N the particle number density and $Re[\cdots]$ indicating the chosen real part. Other polarization components beyond E_x in the establishment of Eq. (4) are safely omitted for simplicity. As we know, for a tightly focusing Gaussian pulse [17,18], other polarization components beyond E_x can be safely neglected if the small correction factor $a_0/Z_R \ll 1$. In our subsequent numerical demonstration, the Rayleigh range is $Z_R \sim 184\,\mu$m if $a_0 = 7\,\mu$m and $\lambda = 0.828\,\mu$m, and thus the condition of $a_0/Z_R \ll 1$ is absolutely satisfied. In addition, as for the propagation distance z considered in this paper, only 350 nm or 8 μm is exemplified, and thus the condition of $Z_R \gg z$ is also satisfied. Therefore one can say a paraxial and plane-wave description of the electric field is in fact enough for our purposes.

The MB equations [Eqs. (3) and (4)] are solved by employing Yee's finite-difference time-domain (FDTD) discretization scheme [19] in combination with the Runge-Kutta method [15,16] or the predictor-corrector algorithm [20–22]. The numerical simulation region boundaries are padded with perfectly matched layers that prevent unphysical

reflections. In the following, for a convenient and direct comparison with Refs. [5,6], similar laser-matter interaction parameters are adopted: $\hbar\omega_0 = 0.5\hbar\omega_{12} = 1.5\,\mathrm{eV}$, $\mu = 0.19\,e\,\mathrm{nm}$, $\tau_0 = 5\,\mathrm{fs}$, $z_0 = -9\,\mu\mathrm{m}$, $a_0 = 7\,\mu\mathrm{m}$, $\varphi = 0$, $N = 2.0 \times 10^{19}\,\mathrm{cm}^{-3}$, and $E_0 = 1.2 \times 10^{10}\,\mathrm{V/m}$ (∼peak intensity of $2.0 \times 10^{13}\,\mathrm{W/cm}^2$). In addition, the medium is initialized with $\rho_{12} = 0$, $n = -1$, and $x_0 = y_0 = 22.5\,\mu\mathrm{m}$.

First, the time evolutions of the few-cycle LG_{10} (i.e., $l = 1$ and $p = 0$) and LG_{00} (i.e., $l = 0$ and $p = 0$) beams at a position of $z = 350\,\mathrm{nm}$ are simulated and shown in Fig. 2. When comparing the laser beams before entering the media, after a short propagation distance of 350 nm, the fields indeed virtually show no visual changes. However, if referring to their spectra [shown in Fig. 1(a)], one can find complicated spectral components beyond the fundamental frequency from the incident fields. Especially, a well-defined spectral peak at twice the incident laser central frequency of ω_0 occurs. As for $l = 0$ and $p = 0$, the spectral distribution is a representation of that given in Ref. [6], where this peak is called a "camouflage" THG, irrespective of its unusual spectral position.

In order to confirm that it is actually a THG process rather than a SHG one, let us turn to another investigation target, i.e., its corresponding transverse electric-field distribution. By utilizing the time-frequency analysis based on the well-known wavelet-transformation technique exemplified by the Gabor transformation with a choice of suitable spectral window widths (here, $0.2\omega_0$ is safely chosen), one can conveniently investigate the transverse field distributions of each harmonic or any certain spectral component. The corresponding results for the unusual SHG at $2\omega_0$ are shown in Figs. 2(c) and 2(d). In Fig. 2(d) the field distribution is a typical Gaussian one for $l = 0$, but, in contrast, from Fig. 2(c), the distribution shows three positive and three negative peaks, a typical LG_{30} mode characteristic. Therefore one can distinguish that the unusual SHG peak at $2\omega_0$ corresponds to a LG_{30} field with a TC number of 3. Then, from the criteria [11–15] that the topological charge number l of a qth-order harmonic is directly proportional to its harmonic order q, $l = ql_0$ with $l_0 = 1$ for a fundamental incident LG_{10} field here, one can say it is in fact a third-order harmonic and not a second-order one. Compared with the mode of characterization used in Refs. [5–7], our scheme seems more direct and easy to implement.

Second, after the above successful demonstration of our characterization scheme, we now investigate the influence of the propagation effects. As shown in Fig. 1(b), after a longer propagation distance of 8 μm, clear and significant distortions to the above unusual SHG occur, where the original peak now becomes a dip as a consequence of significant absorption due to propagation effects. Moreover, the larger the propagation distance, the stronger is the absorption [23]. However, following the same wavelet-transformation scheme above, one can continue to investigate the transverse electric-field distributions (Fig. 3), especially those of the unusual SHG "dip" shown in Fig. 3(b). It still clearly shows a LG_{30} mode characteristic with three positive and three negative peaks, which indicates that its TC number survives from a long-distance propagation and is not destroyed [10]. Beyond this $2\omega_0$ spectral component, the transverse distributions of the first-, third-, and fifth-order vortex harmonics in Figs. 3(a), 3(c), and 3(d) clearly tell us the TC number of a qth-order

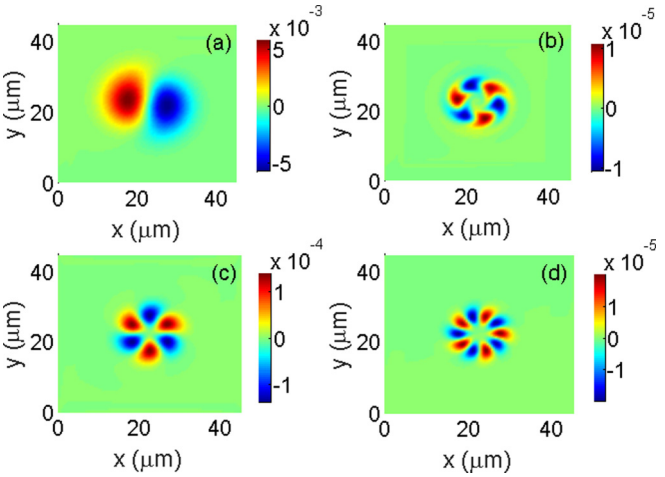

FIG. 3. Transverse field distributions of the (a) first-, (b) unusual "second-," (c) third-, and (d) fifth-order harmonics for LG_{10} field after a propagation distance of 8 μm, obtained via the Gabor transformation with a suitable spectral width of $0.2\omega_0$ at $t = 47$ fs.

harmonic is directly proportional to its harmonic order q. In contrast, for the corresponding transverse electric-field distributions for an incident LG_{00} with a TC number of $l = 0$, typical Gaussian distributions are retained for the first-, second-, and third-order harmonics and also the unusual SHG dip, as shown in Fig. 4. Here, one item we need to point out is that the harmonic generation is attributed to carrier-wave effects, such as carrier-wave Rabi flopping [2] and carrier nonlinearity [15,24], which is a different origin of harmonic generation for multicycle long pulses, which are due to rapid energy-level crossings under very large frequency detuning in two-state laser-matter interaction systems [25,26].

Finally, in the above numerical demonstration, $\omega_{12} = 2\omega_0$ is assumed, for a direct comparison with the results in Refs. [5–7]. In fact, such a two-photon condition is not a requisite. The unusual SHG peak in Fig. 1(a) has been shown to be a THG peak by our characterization scheme and also the other method used in Refs. [5–7]. The origin is the result of a resonant enhancement effect at twice the incident laser frequency from the contribution of the low-energy long tail of the third-order

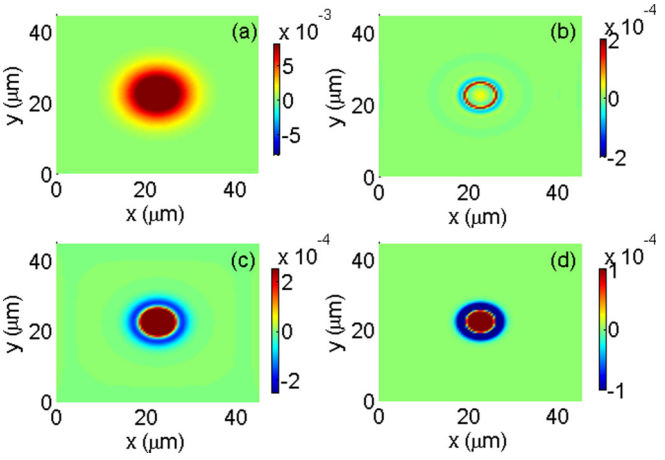

FIG. 4. Same as in Fig. 3, but for a LG_{10} field.

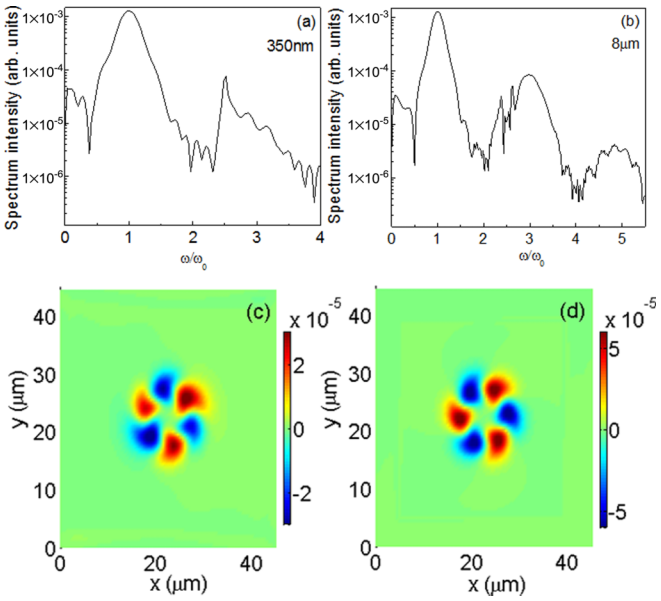

FIG. 5. Upper: Spectra of few-cycle LG pulses with TC $l = 1$ after a propagation distance of (a) 350 nm and (b) 8 μm, respectively. Lower: Transverse field distributions of the unusual spectral components at $2.5\omega_0$ are also presented via the Gabor transformation with a suitable spectral width of $0.2\omega_0$ at (c) $t = 21.5$ fs and (d) $t = 47$ fs.

harmonic. A confirmation of this reasoning can also easily be confirmed if we choose an incident laser frequency ω_0, for example, to let $\omega_{12} = 2.5\omega_0$ be satisfied beyond the condition of $\omega_{12} = 2\omega_0$. As shown in Fig. 5, one will also find a well-defined peak beside the third-order harmonic [Fig. 5(a)], which exactly locates at $2.5\omega_0$. Moreover, it would become a dip after a long enough propagation distance of 8 μm [Fig. 5(b)]. However, the LG_{30} mode characteristics are retained if we turn to their transverse electric-field distributions at $2.5\omega_0$ based on the Gabor transformation [Figs. 5(c) and 5(d)], which indicated this peak is really a third-order harmonic. This demonstration confirms that this unusual peak is actually attributed to the resonant enhancement effect from the long tail of the third-order harmonic.

In conclusion, we have proposed a characterization scheme based on vortex transformation for a recently observed third-harmonic peak that appears to be a second-harmonic peak. Its feasibility is confirmed by a numerical demonstration. The well-defined peak is attributed to a third-harmonic-generation process manifesting itself as a typical transverse electric-field distribution of a LG_{30} mode laser, and thus its origin is directly distinguished based on the criteria that the topological charge number of harmonics is directly proportional to its harmonic order.

This work is supported by National Natural Science Foundation of China (Grants No. 11374318, No. 11674312, and No. 61775087) and Natural Science Foundation of Jiangsu province (No. BK20161159). C.J.Z. gratefully acknowledges the support of Open Fund of the State Key Laboratory of High Field Laser Physics of SIOM. C.P.L. appreciates the support from the 100-talents Project of Chinese Academy of Sciences.

[1] M. Wegner, *Extreme Nonlinear Optics* (Springer, Heidelberg, 2005).
[2] S. Hughes, Phys. Rev. Lett. **81**, 3363 (1998).
[3] C. Van Vlack and S. Hughes, Phys. Rev. Lett. **98**, 167404 (2007).
[4] O. D. Mücke, T. Tritschler, M. Wegener, U. Morgner, and F. X. Kärtner, Phys. Rev. Lett. **87**, 057401 (2001).
[5] T. Tritschler, O. D. Mücke, M. Wegener, U. Morgner, and F. X. Kärtner, Phys. Rev. Lett. **90**, 217404 (2003).
[6] T. Tritschler, O. D. Mücke, U. Morgner, F. X. Kärtner, and M. Wegner, Phys. Status Solidi B **238**, 561 (2003).
[7] O. D. Mücke, T. Tritschler, M. Wegener, U. Morgner, and F. X. Kärtner, Opt. Lett. **27**, 2127 (2002).
[8] A. Mair, A. Vaziri, G. Weihs, and A. Zeilinger, Nature (London) **412**, 313 (2001).
[9] A. Picon, A. Benseny, J. Mompart, J. R. V. de Aldana, L. Plaja, G. F. Calvo, and L. Roso, New J. Phys. **12**, 083053 (2010).
[10] M. Zürch, C. Kern, P. Hansinger, A. Dreischuh, and Ch. Spielmann, Nat. Phys. **8**, 743 (2012).
[11] L. Rego, J. San Román, A. Picón, L. Plaja, and C. Hernández-García, Phys. Rev. Lett. **117**, 163202 (2016).
[12] C. Hernández-García, A. Picón, J. San Román, and L. Plaja, Phys. Rev. Lett. **111**, 083602 (2013).
[13] G. Gariepy, J. Leach, K. T. Kim, T. J. Hammond, E. Frumker, R. W. Boyd, and P. B. Corkum, Phys. Rev. Lett. **113**, 153901 (2014).
[14] X. Zhang, B. Shen, Y. Shi, X. Wang, L. Zhang, W. Wang, J. Xu, L. Yi, and Z. Xu, Phys. Rev. Lett. **114**, 173901 (2015).
[15] Y. Chen, X. Feng, and C. Liu, Phys. Rev. Lett. **117**, 023901 (2016).
[16] V. P. Kalosha and J. Herrmann, Phys. Rev. Lett. **83**, 544 (1999).
[17] C. Liu, M. C. Kohler, K. Z. Hatsagortsyan, C. Müller, and C. H. Keitel, New J. Phys. **11**, 105045 (2009).
[18] Y. I. Salaminm, New J. Phys. **8**, 133 (2006).
[19] K. Yee, IEEE Trans. Antennas Propag. **14**, 302 (1966).
[20] R. W. Ziolkowski, J. M. Arnold, and D. M. Gogny, Phys. Rev. A **52**, 3082 (1995).
[21] C. W. Luo, K. Reimann, M. Woerner, T. Elsaesser, R. Hey, and K. H. Ploog, Phys. Rev. Lett. **92**, 047402 (2004).
[22] C. Zhang, W. Yang, X. Song, and Z. Xu, Phys. Rev. A **79**, 043823 (2009).
[23] B. Macke and B. Ségard, Phys. Rev. A **86**, 013837 (2012).
[24] Y. Xiao, D. N. Maywar, and G. P. Agrawal, Opt. Lett. **38**, 724 (2013).
[25] F. I. Gauthey, B. M. Garraway, and P. L. Knight, Phys. Rev. A **56**, 3093 (1997).
[26] C. Liu, S. Gong, R. Li, and Z. Xu, Phys. Rev. A **69**, 023406 (2004).